

with a C/D ratio of 2. It is as expected that the vertical displacement dominates the soil deformation field in both cases.

For the tunnel with a C/D ratio of 1, the influence zone consists of a rectangle in the upper part and an inverted trapezoid in the lower part. The soil displacement field is very similar to that reported by Potts (1976). The rectangle part is located above the tunnel at about $1/4 D$.

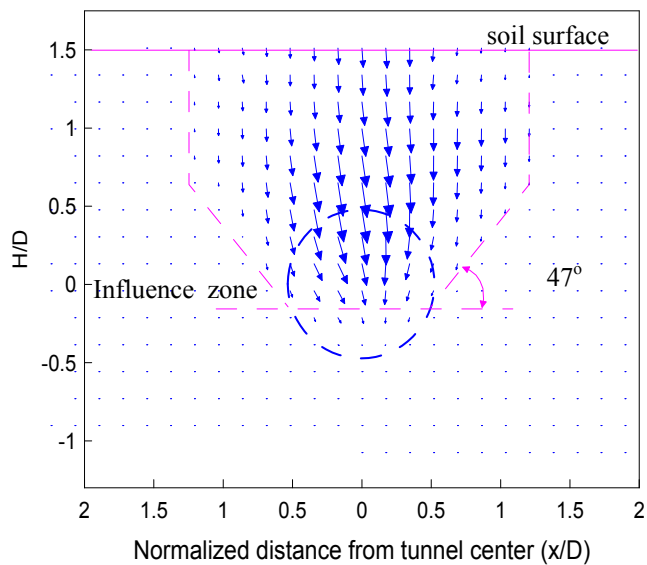
For the tunnel with a C/D ratio of 2, the top rectangular part turns to a bell shape due to soil arching while the bottom trapezoid is almost the same. The top bell part extends about one and a half D above the tunnel crown. It is worthy note that there is minimal deformation at the ground surface. In practice, there will be significant settlement measured at the ground surface for a tunnel with a cover twice the tunnel diameter. The main reason is believed to be the low confining pressure in this scaled model. The influence of soil dilation at this low confining pressure can not accurately represent the stress-dependant behavior of natural soils in the field. This also means that the results from this model study cannot be simply extrapolated and compared to measurements from the field. A surcharge could alleviate the influence from low confining pressure, however, it might also influence the settlement trough. This method was not adopted in this study and is worthy of consideration in the future study. A similarity law is also required to relate the findings to field performance.

The influence zone starts at the tunnel spring line and forms an angle with the horizontal ranging from 47° to 57° . These values are close to the 45° suggested by Loganathan and Poulos (1998). These shapes of influence zone are different from the invert triangle reported by Ahmed and Iskander (2011). The interested section in this study is ahead of TBM, while Ahmed and Iskander (2011) studied the section behind TBM pass-by. The model shield used in this study is also different from the PVC tube method in Ahmed and Iskander (2011). All these can contribute to the discrepancies between two studies.

Internal Soil Displacement Field in Longitudinal Section

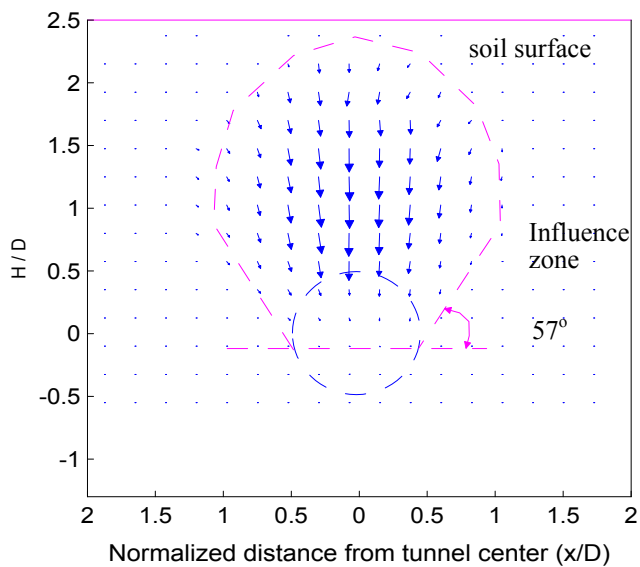
The soil displacement fields along the longitudinal section are shown in Figure 4. Figure 4a is the soil displacement field for the tunnel with a C/D ratio of 1 and Figure 4b for the case with the C/D ratio of 2.

It is as expected that the soil deforms toward the shield machine as it is extracted from its original position to trigger the ground movement. For the tunnel with a C/D ratio of 1, the influence zone consists of a curved zone extending from the tunnel invert to the ground surface and a straight line extending vertically from the TBM crown to the ground surface. The influence zone extends to a distance from the cutter head twice the tunnel diameter as it reaches the ground surface. For the tunnel with a C/D ratio of 2, the curved part extends to a height about one and a half times the tunnel diameter above the tunnel crown and does not extend to the ground surface. This is consistent with the transversal section where the influence zone is confined inside the soil mass.



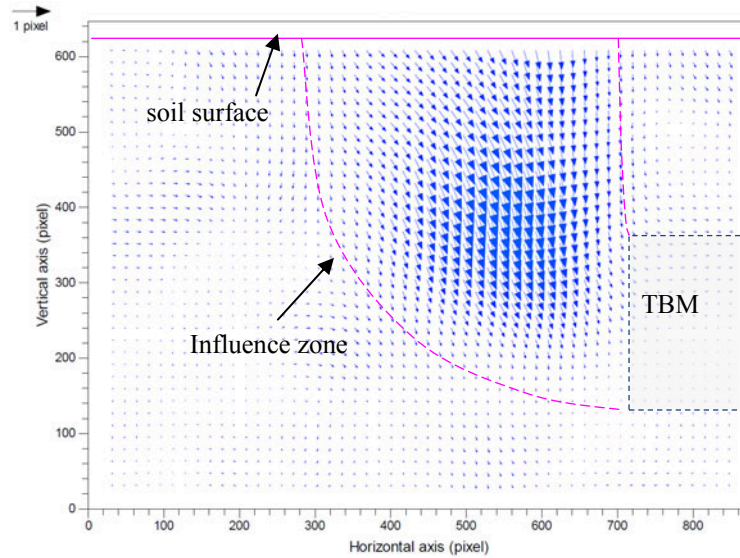
a) The tunnel with a C/D ratio of 1

b)

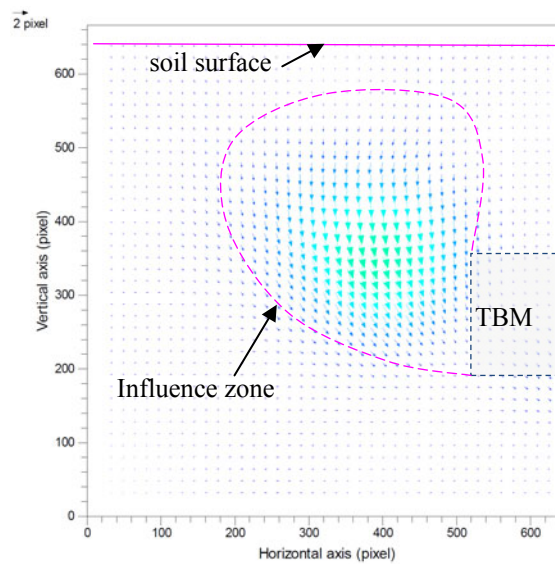


b) The tunnel with a C/D ratio of 2

FIG. 3. Internal soil displacement field observed on a transversal section.



a) The tunnel with a C/D ratio of 1



b) The tunnel with a C/D ratio of 2

FIG. 4. Internal soil displacement field observed on longitudinal section.

CONCLUSIONS AND DISCUSSIONS

A new kind of transparent soil made of fused silica and calcium bromide solution is used in this study to obtain the internal soil deformation on both a transverse section perpendicular to the tunnel axis and a longitudinal section parallel to the tunnel axis. Based on the study, the following conclusions can be drawn:

Transparent soil can be used to visualize internal soil deformation induced by tunneling with the aid of digital image processing techniques. A spatial internal soil

displacement fields for both perpendicular and parallel to the tunnel alignment is obtained in this study.

The influence zone in a shallow tunnel is very different from that in a deep tunnel. The qualitative results obtained from this study are in general agreement with those reported in the literatures.

However, there are limitations in this study. The tests are performed in a scaled model at the gravity condition. The stress-dependent behavior of natural soils cannot be modeled properly in this study. The results from this scaled model cannot be simply proportioned to relate to field measurement. The soil deformation is triggered by extracting the model shield in this study. A more realistic shield machine model can be used in the future. The transparency of the model degrades gradually with increasing size of the model. This issue restrains the use of a larger model, which causes some boundary effect, particularly in the deep tunnel case. A high purity fused silica and a fluid with a better match of refractive indices should be investigated for future studies.

ACKNOWLEDGMENTS

The authors want to acknowledge the financial support from the State Key Laboratory of Geomechanics and Geotechnical Engineering of China for this study.

REFERENCES

- Ahmed, M. and Iskander, M. (2011). "Evaluation of tunnel face stability by transparent soil models." *Tunnelling & Underground Space Tech.* 27, 101–110.
- Holtz, H.D., Kovacs, W.D., and Sheahan, T.C. (2011). *An Introduction to Geotechnical Engineering*, 2nd edition, Prentice Hall.
- Kirsch, A. (2010). "Experimental investigation of the face stability of shallow tunnels in sand." *Acta Geotechnica*, 5, 43–62.
- Leca, E. and Clough, G.W. (1992). "Preliminary design for NATM tunnel support in soil." *J. of Geot. Eng. Div.*, ASCE, 118 (4), 558–575.
- Loganathan N. and Poulos, H · (1998). "Analytical prediction for tunneling-induced ground movement in clays." *J. of Geot. & Geoenv. Eng.*, 124(9): 846-856.
- Mair R.J., Taylor, R.N., and Bracegirdle, A. (1993). "Subsurface settlement profiles above tunnels in clays." *Geotechnique*, 43(2), 315-320.
- Meguid, M.A., Saada, O., Nunes, M.A., and Mattar, J. (2008). "Physical modeling of tunnels in soft ground: a review." *Tunnel. & Underground Space Tech.*, 23, 185–198.
- Nomoto, T., Imamura, S., Hagiwara, T., Kusakabe, and O., Fujii, N. (1999). "Shield tunnel construction in centrifuge." *J. of Geot. & Geoenv. Eng.*, 125 (4), 289–300.
- O'Reilly, M. P. and New, B. M. (1982). "Settlements above tunnels in the UK- Their magnitude and prediction." *Proceedings, Tunneling'82*, London, 173-181.
- PIVTEC GMBH (2006). *PIVview User Manual*, Ver.2.4, <http://www.pivtec.com/>.
- Peck, R.B. (1969). "Deep excavations and tunneling in soft ground." *Proc. 7th ICSMFE*, Mexico City, 225–290.
- Potts, D.M. (1976). "Behaviour of lined and unlined tunnels in sand." *Ph.D. Dissertation*, University of Cambridge, UK.

Experimental Study on Improving the Frost Heave of Graded Gravel on Passenger Dedicated Railway Line

Zhi-Hong Nie¹, Yuan Liu and Xiang Wang

¹Associate Professor, School of Civil Engineering, Central South University, Changsha, Hunan 410075, China; niezhih@126.com

ABSTRACT: Frost heave significantly affects the graded gravel used to construct passenger-dedicated railway lines. For safety reasons, such lines have strict demands on the amount of deformation that can occur to tracks. The aim of this study was to investigate the geotechnical properties of graded gravel that was grouted with slurry. After grouting, scanning electron microscopy showed that the slurry bound well to the gravel particles. With increasing iterations of freeze-thaw cycles, the frost heave ratio increased, but it did not change significantly after 20 freeze-thaw cycles. In addition, changes in the unconfined compression strength were also negligible after 20 freeze-thaw cycles, and they tended to stabilize after 10 dry-wet cycles. These results show that graded gravel samples stabilized with slurry exhibited high resistance to the effects of freeze-thaw cycles and dry-wet cycles. We concluded that slurry can be successfully used to improve frost heave associated with the graded gravel of passenger-dedicated railway line.

INTRODUCTION

Frost heave problems in subgrade of passenger dedicated lines have been discovered in northern of China. In winter, frost heave of the subgrade produces uneven deformation, and this uneven surface causes deterioration of the subgrade cracking (Seppala 1999). Freeze-thaw cycles lead to frost boils and deformation of the subgrade when traffic loads are applied, severely hindering normal operation of the railway line. According to field observations, 90% of the frost heave is produced in the surface layer of the subgrade. Because it is a key part of the surface layer, graded gravel in the subgrade is especially affected by frost heave.

Moisture is generally considered one of the most important factors that influence frost heave in soils. Compared with water, grout shows better affinity with soil. In certain negative pressure conditions, slurry was grouted into the soil, which then fills the pores and reduces the moisture in the graded gravel. The slurry forms a solid with the graded gravel, which prevents the surface water from penetrating into the soil after improved, and thereby reduces the water content in the graded gravel as well.

So far, few studies have investigated frost heave of coarse-grained soils. Vinson et al. (1986) concluded that particle size must be considered when

developing the criteria for determining frost heave susceptibility. Zhang et al. (2007) studied the relationship between the frost heave ratio and they revealed that coarse-grained soils regularly undergo frost heave.

Several studies have studied the properties of modified soils in freeze-thaw cycles. Yarbasi et al. (2007) indicated that waste materials can be used as additives to enhance the freeze-thaw durability of granular soils. In addition, Kalkan(2009) demonstrated that the unconfined compressive strength and permeability of fine-grained soil samples stabilized with silica fume are resistant to the effects of freeze-thaw cycles. Liu et al. (2010) investigated the dynamic properties of cement- and lime-modified clay soils that were subjected to freeze-thaw cycles. Their results showed that the modified soils exhibited better performance than unmodified soils.

The main objective of this study was to investigate graded gravel after grouting to determine if grouting can reduce the effects of permeability and frost heave. At the same time, we explored slurry as a stabilization material to reduce the effects of freeze-thaw cycles and dry-wet cycles on strength.

MATERIALS & METHODS

Graded gravel

For this study, graded gravel was supplied from Dalian, in northeastern China. The maximum dry density of graded gravel was 2.24g/cm³. The grain-size distribution of graded gravel is given in Fig.1. The X-ray diffraction (XRD) patternof the graded gravel is shown in Table 1.

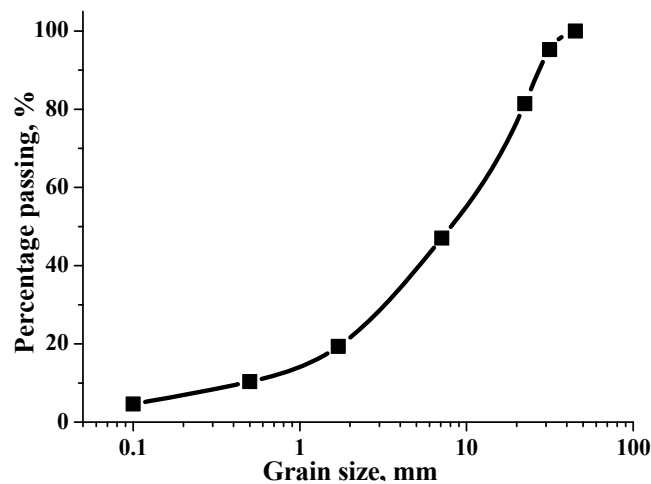


FIG. 1. The grain-size distribution of graded gravel in natural conditions

Table 1.X-ray diffraction (XRD) pattern of graded gravel

Compound	Quartz	Calcite	Dolomite	Mica	Kaolinite	Feldspar
Content (%)	5.72	71.76	14.54	1.97	1.85	4.16

Slurry

The density of slurry was 1.11 g/cm³. The main ingredients and mixing proportion of the slurry was as follows: A liquid: catalyst 1: catalyst 2: brine=100 : 3 : 2 : 1. The technical index of the grouting material is summarized in Table 3.

Table 3. Technical index of grouting material

Density (g/cm ³)	Viscosity (MPa·s)	Coagulation time (hours)	Cured strength (MPa)
1.11	1.20	4.5	0.25

Sample preparation

After the samples were prepared, an appropriate amount of slurry was injected into each specimen from the bottom of the sample using a grouting tube. Samples used in the unconfined compression strength tests had dimensions of 100 mm in diameter and 100 mm in length. Samples for frost heave tests were 156mm in diameter and 110 mm in length. In these tests, at least 3 samples were prepared for each combination of variables. The modified samples are shown in Fig. 2, where scanning electron image showed that the particles bound well with the slurry.



FIG. 2. Scanning electron image of the improved graded gravel.

Experimental study

The falling head permeability test apparatus used a 70-mm head permeameter. The tests were conducted in accordance with the Code for Soil Tests of Railway Engineering (TB10102-2010). The permeability coefficient was calculated as the following equation:

$$k_T = QL / AHt \tag{1}$$

$$k_{20} = k_T \eta_T / \eta_{20} \tag{2}$$

where k_T and k_{20} are the permeability coefficients at water temperatures of $T^\circ\text{C}$ and 20°C , respectively. The Q is the volume of water that leaves the permeameter in t

seconds; A is the area of the sample in square centimeters; L is the length between the piezometric tubes; t is the elapsed time in seconds; H is the average water head; and η_T and η_{20} are the dynamic viscosities of water at $T^\circ\text{C}$ and 20°C , respectively.

Frost heave tests were carried out in accordance with Code for Soil Tests of Railway Engineering (TB10102-2010). For the tests, 3 replicates (156 mm in diameter and 110 mm in length) were performed for each test. The frost heave ratio was calculated according to the following equation:

$$\eta = \Delta h / H \cdot 100\% \tag{3}$$

where η is the frost heave ratio of the sample, Δh is the change in length of the sample in centimeters, and H is the original length of the specimen (110mm).

The tests were carried out to determine the unconfined compression strength of the samples in accordance with the Code for Soil Tests of Railway Engineering (TB10102-2010). A total of 3 samples were tested in each group, and all of these samples were tested at a deformation rate of 1mm/min.

To freeze the specimens, they were placed at -20°C for 4h. After freezing, the samples were placed at 20°C for 4h. Then the frost heave ratio and unconfined compression strength of each sample were tested after freeze-thaw cycles.

During dry-wet cycles, the samples (grouted with slurry) were totally immersed in water for 24 h, and then they were removed and allowed to dry for 24h under laboratory conditions. The grouted samples were performed unconfined compression testing in certain times dry-wet cycles .

RESULTS & DISCUSSION

Effect of slurry on the permeability

A linear correlation was calculated between the void ratio and the logarithm of the permeability coefficient of graded gravel, and the results are depicted in Fig.3.

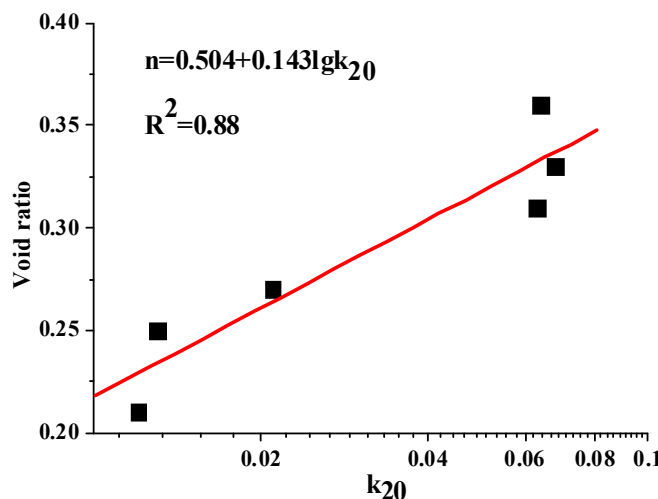


FIG. 3. Relationship between the void ratio and the permeability coefficient.

The relationship between the void ratio and the permeability coefficient is given by the following equation: $n = 0.504 + 0.143 \lg k_{20}$ ($r^2 = 0.88$) where n is the void ratio of graded gravel and k_{20} is the permeability coefficient at a

water temperature of 20°C. After grouting, the permeability of samples was 1.410×10^{-10} cm/s, which was significantly lower than that was not grouted.

Because the slurry filled voids in the samples, the void ratio of graded gravel after grouting decreased. With this decrease in void ratio, the permeability of samples also decreased significantly after modification.

Effect of slurry on the frost heave ratio after freeze-thaw cycles

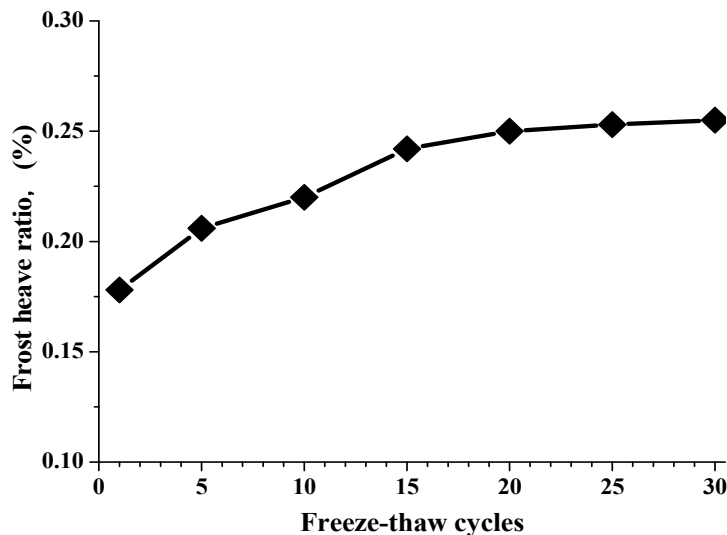


FIG. 4. Effect of grouting on the frost heave ratio in freeze-thaw cycles.

Results of the frost heave ratio tests are shown in Fig.4. The frost heave ratio of samples increased with increasing numbers of freeze-thaw cycles, and the maximum frost heave ratio of samples was 0.250%. After the number of freeze-thaw cycles reached 20, the frost heave ratio of specimens tended not to change further.

The volume of frozen moisture increases in soil as the temperature drops below 0°C, and the forming ice crystals extrude into the nearby soil and destroy the soil structure. The soil eventually settles as thawing occurs and the ice crystals melt when the temperature increases. In dense soils, the void ratio increases with the number of freeze-thaw cycles (Viklander 1998 and Qi et al. 2005). In the study, frost heave and the soil thawing process were not fully reversible, and the amount of frost heave exceeded the amount of soil settlement that occurred during thawing in the freeze-thaw cycles. The structure of the soil gradually stabilized as freeze-thaw cycles increased, at which time the frost heave ratio of the soil changed negligibly.

After the soil was improved, the void ratio was significantly reduced and the moisture content was low. The slurry filled in the granule and worked as a buffer to reduce the effects of freeze-thaw cycles on the modified graded gravel.

Effect of slurry on the unconfined compression strength

After the freeze-thaw cycles

The effect of freeze-thaw cycles on the unconfined compression strength of the samples is shown in Fig.5. This figure shows that the unconfined compression

strength of samples decreased from 3.61 to 2.40MPa after 20 freeze-thaw cycles. Subsequently, the unconfined compression strength stabilized.

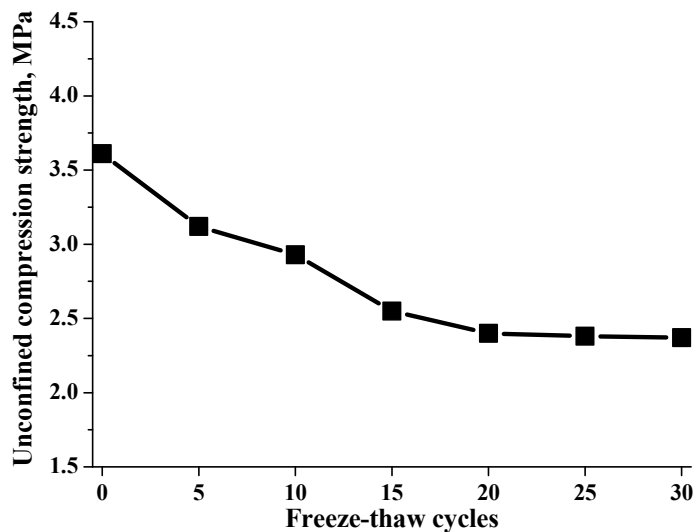


FIG. 5. Effect of freeze-thaw cycles on unconfined compression strength.

When it freezes, the volume of moisture expands (about 9%) in soil, and the ice crystals extrude into the soil and its surroundings. As a result, mutual movements occur and the spaces between soil particles increase. During thawing, the soil settles and the amount of unfrozen moisture in the soil increases as the frozen moisture melts. In this case, the soil particles move again and the moisture acts as a lubricant. These destructive effects accumulate as the number of freeze-thaw cycles increases, and the decreases in unconfined strength can be attributed to particle rearrangements and microstructures that are damaged by freeze-thaw cycles (Kalkan 2009).

The fine particles were trapped in the slurry after grouting, and the interactions between the fine particles and water were visibly reduced. When the ice crystals extruded into the soil, the grouting material exhibited a certain degree flexibility acting as a buffer.

After the dry-wet cycles

The results of the unconfined compression strength tests after dry-wet cycles are depicted in Fig.6. The unconfined compression strength decreased gradually as the number of dry-wet cycles increased. The unconfined compression strength decreased from 3.61 to 2.61 MPa after samples were exposed to 10 dry-wet cycles; subsequently, the unconfined compression strength did not change.

The humidity of soil increases when it is immersed in water. The water film between soil particles becomes thick, and the skeletons of soil particles expand after binding with the moisture. However, the addition of cement causes the soil particles to rearrange. The moisture content decreases and the soil skeletons shrink after drying, again disturbing the soil structure (Zhao and Wang 2012). With the increasing number of dry-wet cycles in our study, the soil structure was continuously destroyed and the soil strength was reduced.